



# Numerical Prediction of Parametric Roll Resonance in Oblique Waves

Naoya Umeda, *Osaka University* [umeda@naoe.eng.osaka-u.ac.jp](mailto:umeda@naoe.eng.osaka-u.ac.jp)

Naoki Fujita, *Osaka University* [naoki\\_fujita-0210@i.softbank.jp](mailto:naoki_fujita-0210@i.softbank.jp)

Ayumi Morimoto, *Osaka University* [cubx1520@gmail.com](mailto:cubx1520@gmail.com)

Masahiro Sakai, *Osaka University* [masahiro\\_sakai@naoe.eng.osaka-u.ac.jp](mailto:masahiro_sakai@naoe.eng.osaka-u.ac.jp)

Daisuke Terada, *National Research Institute of Fisheries Engineering*, [dterada@fra.affrc.go.jp](mailto:dterada@fra.affrc.go.jp)

Akihiko Matsuda, *National Research Institute of Fisheries Engineering*, [amatsuda@fra.affrc.go.jp](mailto:amatsuda@fra.affrc.go.jp)

## ABSTRACT

Numerical prediction of parametric roll in head and following waves has been intensively investigated so that requirements for reasonably good prediction are almost revealed. On the other hand, prediction of parametric roll in oblique waves has not yet been sufficiently established. This is because coupling with sway and yaw motions are unavoidable. Since parametric roll for actual ships occurs with very low forward velocity, even accurate prediction of lee ways in waves is not so easy. Therefore, in this study, the authors present a numerical model of parametric roll in oblique waves with low-speed manoeuvring forces taken into account. Then the numerical prediction was compared with newly executed free-running model experiments of a hypothetical ship. Its results demonstrate the present model shows reasonably good agreement with the experiment. This information could be used for identifying minimum requirements for good prediction of parametric roll in oblique waves.

**Keywords:** *parametric rolling, IMO, Second generation intact stability criteria, direct stability assessment, operational guidance*

## 1. INTRODUCTION

Although danger of parametric rolling had been well known among scientists (e.g. Watanabe, 1934), the accident of a C11 class post Panamax containership (France, 2003) induced extensive studies on this phenomenon. As a result, several numerical models for parametric rolling were developed and some of them were well validated with model experiments in head and following waves (Reed, 2011). These models deal with coupled heave-pitch-roll motions by using simultaneous nonlinear differential equations and the hydrodynamic coefficients used in the equations are calculated with potential theories

and empirical viscos force estimation. Time dependence of roll restoring coefficient, including coupling from other modes and diffraction moment depending on heel angle, is indispensable.

Based on such progress in research for parametric rolling, at the International Maritime Organisation (IMO), stability criteria for preventing parametric roll is now under development (Umeda, 2013). They consist of three layers: the first and second layers use simplified estimation of occurrence and magnitude of parametric roll in head and following waves with averaging method applied to uncoupled roll model with restoring variation; the third layer means direct use of numerical simulation in time domain of

coupled roll model in irregular waves. For the latter case, the numerical models mentioned before could be used. It is noteworthy here that the third layer requires not only calculation in head and following waves but also in oblique waves. This is because we have to evaluate safety for all ship courses. For oblique waves, validation efforts for existing numerical models (Sanchez & Nayfeh, 1990; Neves & Valerio, 2000) were not sufficient so far partly because a model experiment requires a seakeeping and manoeuvring basin and partly because coupling with manoeuvring motion including rudder actions are unavoidable.

Based on this understanding, the authors attempted to validate a numerical simulation model taking low-speed manoeuvring model in oblique waves with a newly executed model experiment in a seakeeping and manoeuvring basin. This numerical model is an extension of the model published in Hashimoto and Umeda (2011) for head and following waves, which were well validated with model experiments of containerships and a car carrier in the towing tank of Osaka University. The ship used in this paper is a typical ship having large flare and transom stern, i.e. a hypothetical ship known as the ONR flare topside vessel, of which hull form is open for public. At this stage comparisons in regular oblique waves are ready to be published. Comparisons in irregular oblique waves are a task for future. In this paper, details of the numerical model are described for facilitating development of the guidelines for the direct assessment at the IMO.

## 2. NUMERICAL MODEL FOR PARAMETRIC ROLL IN OBLIQUE WAVES

### 2.1 Coordinate systems and equations of coupled motions

The coordinate systems used here are shown in Figure 1. The space-fixed coordinate system is  $O_1-\xi\eta\zeta$ , the coordinate system

moving with a constant speed of  $U$  and course of  $\chi$  is  $O_2-XYZ$  and the body-fixed coordinate system is  $G-xyz$ . Here we assume that a wave propagates in the direction of  $O_1\xi$  axis. The ship oscillates around the  $O_2-XYZ$ .  $G$  indicates the centre of ship mass and  $O_1G_0$  indicates initial depth of centre of ship mass. The ship motions around the  $O_2-XYZ$  are denoted by  $x_i$ : surge ( $i=1$ ), sway ( $i=2$ ), heave ( $i=3$ ), roll ( $i=4$ ), pitch ( $i=5$ ) and yaw ( $i=6$ ).

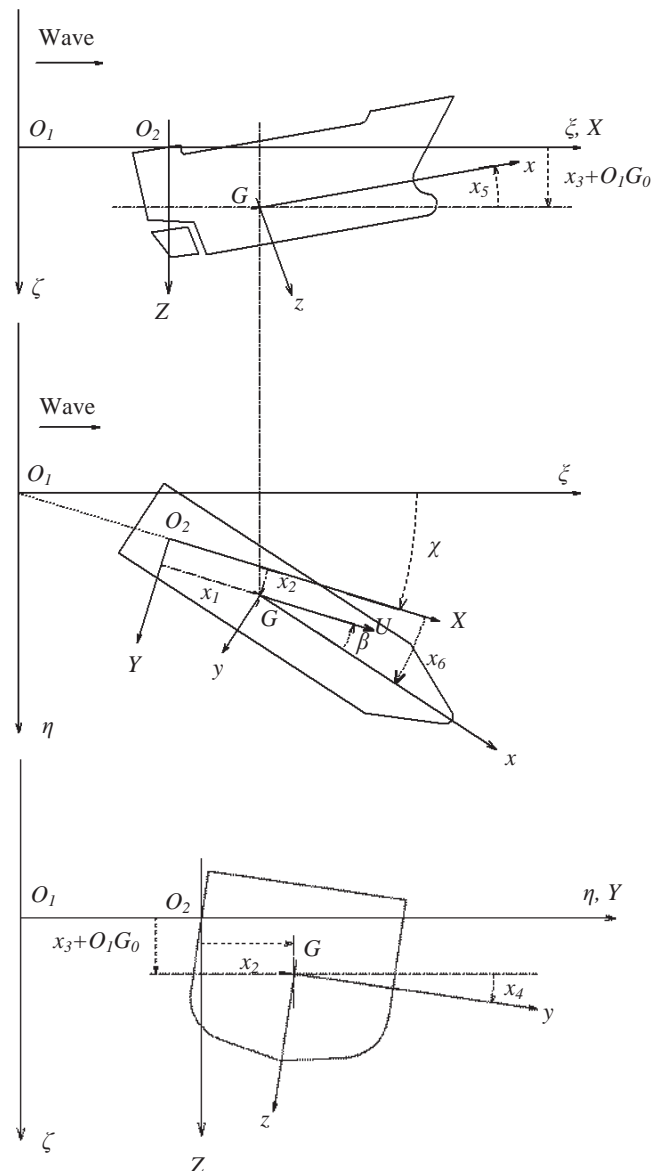


Figure 1 Coordinate systems

The coupled sway-heave-roll-pitch-yaw motions are modelled as follows:



$$\begin{cases} m\ddot{x}_2 = F_2(x_2, x_3, x_4, x_5, x_6, \dot{x}_2, \dot{x}_3, \dot{x}_4, \dot{x}_5, \dot{x}_6, \ddot{x}_2, \ddot{x}_3, \ddot{x}_4, \ddot{x}_5, \ddot{x}_6, t) \\ m\ddot{x}_3 = F_3(x_2, x_3, x_4, x_5, x_6, \dot{x}_2, \dot{x}_3, \dot{x}_4, \dot{x}_5, \dot{x}_6, \ddot{x}_2, \ddot{x}_3, \ddot{x}_4, \ddot{x}_5, \ddot{x}_6, t) \\ I_{xx}\ddot{x}_4 = F_4(x_2, x_3, x_4, x_5, x_6, \dot{x}_2, \dot{x}_3, \dot{x}_4, \dot{x}_5, \dot{x}_6, \ddot{x}_2, \ddot{x}_3, \ddot{x}_4, \ddot{x}_5, \ddot{x}_6, t) \\ I_{yy}\ddot{x}_5 = F_5(x_2, x_3, x_4, x_5, x_6, \dot{x}_2, \dot{x}_3, \dot{x}_4, \dot{x}_5, \dot{x}_6, \ddot{x}_2, \ddot{x}_3, \ddot{x}_4, \ddot{x}_5, \ddot{x}_6, t) \\ I_{zz}\ddot{x}_6 = F_6(x_2, x_3, x_4, x_5, x_6, \dot{x}_2, \dot{x}_3, \dot{x}_4, \dot{x}_5, \dot{x}_6, \ddot{x}_2, \ddot{x}_3, \ddot{x}_4, \ddot{x}_5, \ddot{x}_6, t) \end{cases} \quad (1)$$

where  $m$ : ship mass,  $I_{xx}$ : moment of inertia of ship mass in roll,  $I_{yy}$ : moment of inertia of ship mass in pitch,  $I_{zz}$ : moment of inertia of ship mass in yaw,  $t$ : time and  $F_j$ : force or moment in the  $j$  direction. A dot denotes differentiation with time. Here we assume that the surge motion  $x_1$  is zero, for avoiding estimation of added mass, so that the ship runs with a constant velocity and a straight course. The forces are modelled with Equation (2).

$$F_j = F_j^R + F_j^B + F_j^{FK} + F_j^D + F_j^{EG} + F_j^{MLS} + F_j^{DEL} \quad (2)$$

where the superscript R indicates the radiation component, B the component due to hydrostatic pressure, FK the component due to incident wave pressure, D the diffraction component, EG component due to gravity, MLS the hull force due to manoeuvring motion and DEL the force due to rudder action.

## 2.2 Buoyancy and Froude-Krylov Forces

If we assume incident waves are sinusoidal, their profile,  $\zeta_w$ , and wave pressure,  $p$ , are given by Equations (3-4).

$$\zeta_w = \zeta_a \cos\left(\frac{\omega_k}{g} \xi - \omega_k t\right) \quad (3)$$

$$p = \rho g \zeta_a \exp\left(-\frac{\omega_k}{g} (\zeta - \zeta_w)\right) \cos\left(\frac{\omega_k}{g} \xi - \omega_k t\right) \quad (4)$$

where  $\rho$ : water density,  $\zeta_a$ : wave amplitude,  $g$ : gravitational acceleration,  $\omega_k$ : wave circular frequency and  $t$ : time. Here water pressure is adjusted to be zero at the wave surface

although this is a higher order correction under the assumption of small wave steepness.

Then submerged hull surface,  $S_H$ , can be determined with Equation (5).

$$S_H = S_H(\zeta_G, \zeta_w, x_3, x_4, x_5) \quad (5)$$

By integrating the water pressure on the wetted hull surface, the buoyancy,  $F_j^B$ , and Froude-Krylov forces,  $F_j^{FK}$ , can be calculated as follows:

$$F_j^B = \rho g \int_L dx \int_{S_H} -\zeta n_j ds \quad (6)$$

$$F_j^{FK} = -\int_L \int_{S_H} p n_j ds dx \quad (7)$$

where  $L$  indicates the range of hull in  $x$  direction. The gravitational force,  $F_3^{EG}$ , in the vertical direction are given by

$$F_3^{EG} = mg \quad (8)$$

## 2.3 Radiation and Diffraction Forces

The radiation force,  $F_i^R$ , can be calculated as follows:

$$F_i^R = \sum_{j=2}^6 (-A_{ij}(x_4) \ddot{x}_j - B_{ij}(x_4) \dot{x}_j - C_{ij}(x_4) x_j) \quad (9)$$

where the added mass,  $A_{ij}$ , the wave damping coefficient,  $B_{ij}$ , and the restoring coefficient,  $C_{ij}$ , are given by

$$A_{22} = \int_L A_{H22} dx, \quad A_{23} = \int_L A_{H23} dx, \quad A_{24} = \int_L A_{H24} dx$$

$$A_{25} = -\int_L x A_{H23} dx, \quad A_{26} = \int_L x A_{H22} dx$$

$$A_{32} = \int_L A_{H32} dx, \quad A_{33} = \int_L A_{H33} dx, \quad A_{34} = \int_L A_{H34} dx$$

$$A_{35} = -\int_L x A_{H33} dx, \quad A_{36} = \int_L x A_{H32} dx$$

$$A_{42} = \int_L A_{H42} dx, \quad A_{43} = \int_L A_{H43} dx$$



$$A_{45} = -\int_L xA_{H43}dx, A_{46} = \int_L xA_{H42}dx$$

$$A_{52} = -\int_L xA_{H32}dx, A_{53} = -\int_L xA_{H33}dx$$

$$A_{54} = -\int_L xA_{H34}dx$$

$$A_{55} = \int_L x^2 A_{H33}dx, A_{56} = -\int_L x^2 A_{H32}dx$$

$$A_{62} = \int_L xA_{H22}dx, A_{63} = \int_L xA_{H23}dx, A_{64} = \int_L xA_{H24}dx$$

$$A_{65} = -\int_L x^2 A_{H23}dx, A_{66} = \int_L x^2 A_{H22}dx$$

$$B_{22} = \int_L B_{H22}dx, B_{23} = \int_L B_{H23}dx, B_{24} = \int_L B_{H24}dx$$

$$B_{25} = -\int_L xB_{H23}dx + U \int_L A_{H23}dx$$

$$B_{26} = \int_L xB_{H22}dx - U \int_L A_{H22}dx$$

$$B_{32} = \int_L B_{H32}dx, B_{33} = \int_L B_{H33}dx, B_{34} = \int_L B_{H34}dx$$

$$B_{35} = -\int_L xB_{H33}dx + U \int_L A_{H33}dx$$

$$B_{36} = \int_L xB_{H32}dx - U \int_L A_{H32}dx$$

$$B_{42} = \int_L B_{H42}dx, B_{43} = \int_L B_{H43}dx,$$

$$B_{45} = -\int_L xB_{H43}dx + U \int_L A_{H43}dx$$

$$B_{46} = \int_L xB_{H42}dx - U \int_L A_{H42}dx$$

$$B_{52} = -\int_L xB_{H32}dx - U \int_L A_{H32}dx$$

$$B_{53} = -\int_L xB_{H33}dx - U \int_L A_{H33}dx$$

$$B_{54} = -\int_L xB_{H34}dx - U \int_L A_{H34}dx$$

$$B_{55} = \int_L x^2 B_{H33}dx, B_{56} = -\int_L x^2 B_{H32}dx + U \int_L xA_{H32}dx$$

$$B_{62} = \int_L xB_{H22}dx - U \int_L A_{H22}dx$$

$$B_{63} = \int_L xB_{H23}dx + U \int_L A_{H23}dx$$

$$B_{64} = \int_L xB_{H24}dx + U \int_L A_{H24}dx$$

$$B_{65} = -\int_L x^2 B_{H23}dx, B_{66} = \int_L x^2 B_{H22}dx$$

$$C_{25} = U \int_L B_{H23}dx, C_{26} = -U \int_L B_{H22}dx$$

$$C_{35} = U \int_L B_{H33}dx$$

$$C_{45} = U \int_L B_{H43}dx$$

$$C_{46} = -U \int_L B_{H42}dx$$

$$C_{55} = -U \int_L xB_{H33}dx - U^2 \int_L A_{H33}dx$$

$$C_{56} = U \int_L xB_{H32}dx + U^2 \int_L A_{H32}dx$$

$$C_{65} = U \int_L xB_{H23}dx + U^2 \int_L A_{H23}dx$$

$$C_{66} = -U \int_L xB_{H22}dx - U^2 \int_L A_{H22}dx$$

$$A_{Hij} - i \frac{B_{Hij}}{\omega} = -\rho \int_{S_H} \varphi_j n_i ds$$

Here  $\varphi_j$  and  $n_i$  are the velocity potential of two-dimensional flow with hull and linear free surface condition and normal vector to the hull surface. The added mass and damping in roll are estimated as follows:

$$I_{xx} + A_{44} = W \cdot GM \left( \frac{T_\phi}{2\pi} \right)^2 \quad (10)$$

$$B_{44} \dot{x}_4 = \alpha \dot{x}_4 + \beta |\dot{x}_4| \dot{x}_4 + \gamma \dot{x}_4^3 \quad (11).$$

The  $\alpha$ ,  $\beta$ ,  $\gamma$  and  $T_\phi$  can be estimated with roll decay test of a ship model.

The diffraction force,  $F_j^D$ , can be calculated as follows (Salvesen et al., 1970):

$$F_j^D = \zeta_a F_{kj}^D(x_4) \cos(-\omega_e t - \varepsilon_{kj}^D(x_4)) \quad (12)$$

where

$$F_{kj}^D = |E_{kj}^D|$$



$$\varepsilon_{kj}^D = \arg E_{kj}^D$$

$$E_{kj}^D = \frac{\rho g \zeta_a}{i\omega} \int_L \int_{S_H} (i\omega_k - U \frac{\partial}{\partial x}) \varphi_D n_j ds$$

$$\omega_e = \omega_k - (\omega_k^2 / g) U \cos \chi$$

And  $\varphi_D$  is the diffraction velocity potential of two-dimensional flow with hull and linear free surface condition in incident waves.

## 2.4 Manoeuvring Forces

Since parametric roll occurs at low speed, it is desirable to estimate manoeuvring forces with a mathematical model suitable for such situation where ship forward velocity is comparable to ship lateral velocity (Umeda & Yamakoshi, 1989). The hull manoeuvring forces,  $F_i^{MLS}$ , can be estimated as the sum of linear lift components,  $Y_L$  and  $N_L$ , and nonlinear cross-flow drag components,  $Y_C$  and  $N_C$ , as follows:

$$F_2^{MLS} = Y_C + Y_L$$

$$F_6^{MLS} = N_C + N_L \quad (13)$$

where

$$Y_C = \frac{1}{2} \rho \int_{-L/2}^{L/2} d \cdot C_D |v + rx| (v + rx) dx$$

$$N_C = \frac{1}{2} \rho \int_{-L/2}^{L/2} d \cdot C_D |v + rx| (v + rx) x dx$$

$$Y_L = Y_v v + Y_r r$$

$$N_L = N_v v + N_r r$$

$$u = (U + \dot{x}_1) \cos x_6 + \dot{x}_2 \sin x_6$$

$$v = -(U + \dot{x}_1) \sin x_6 + \dot{x}_2 \cos x_6$$

$$r = \dot{x}_6$$

$$Y_v = \left( \frac{1}{2} \rho L_{pp} d \cdot u \right) \cdot Y_v'$$

$$N_v = \left( \frac{1}{2} \rho L_{pp}^2 d \cdot u \right) \cdot N_v'$$

$$Y_r = \left( \frac{1}{2} \rho L_{pp}^2 d \cdot u \right) \cdot Y_r'$$

$$N_r = \left( \frac{1}{2} \rho L_{pp}^3 d \cdot u \right) \cdot N_r'$$

Here  $u$  and  $v$  are the surge and sway velocity defined with the body-fixed coordinate system G-xyz, respectively.  $C_D$  is the cross-flow drag coefficient when the ship is laterally towed.

The rudder-induced forces,  $F_i^{DEL}$ , are calculated as follows:

$$F_2^{DEL} = -(1 + a_H) \frac{1}{2} \rho A_R u_R^2 f_\alpha \delta$$

$$F_6^{DEL} = -(x_R + a_H x_H) \frac{1}{2} \rho A_R u_R^2 f_\alpha \delta \quad (14)$$

where

$$\delta = -K_p x_6$$

$$u_R = \varepsilon u_p \sqrt{1 + \frac{8K_T}{\pi J^2}}$$

$$u_p = (1 - w_p) U$$

$$J = \frac{u_p}{nD_p}$$

$$K_T = aJ^2 + bJ + c$$

$$u_R = \varepsilon u_p \sqrt{1 + \frac{8}{\pi} \left( a + \frac{b}{J} + \frac{c}{J^2} \right)}$$

$$= \varepsilon u_p \sqrt{1 + \frac{8}{\pi} \left( a + \frac{bnD}{u_p} + \frac{cn^2 D^2}{u_p^2} \right)}$$

$$= \varepsilon u_p \sqrt{u_p^2 + \frac{8}{\pi} (a u_p^2 + bnD u_p + cn^2 D^2)}$$

Here  $\delta$ : rudder angle,  $a_H$ : the interaction factor for rudder force between hull and rudder,  $x_H$ : the longitudinal position of rudder force due to

interaction between hull and rudder,  $x_R$ : the longitudinal rudder position,  $A_R$ : the rudder area,  $f_\alpha$ : the hydrodynamic rudder lift slope,  $K_P$ : the rudder gain,  $n$ : the propeller revolution number,  $D_P$ : the propeller diameter,  $K_T$ : the rudder gain,  $\varepsilon$ : the wake ratio between propeller and rudder. The flow straightening effect is ignored.

The system parameters for manoeuvring forces and moments, such as  $C_D$  and  $Y_v$ , can be estimated with captive model experiment of a ship. In this paper, we used the coefficients measured in the circular motion tests of the C11 class post Panamax containership, whose hull form is similar to the ONR flare topside vessel.

### 3. MODEL EXPERIMENTS

For validating a numerical model for parametric rolling in oblique waves, experiments using a 1/48.8 scaled model of the 154m-long ONR flare topside vessel were executed at the seakeeping and manoeuvring basin of National Research Institute of Fisheries Engineering, based on the ITTC recommended procedure on intact stability model test (ITTC, 2008). The ship was propelled with an electric motor and two propellers and steered with two rudders. The propeller RPM was controlled to be a constant and the auto pilot was used with the rudder gain of 1.0. The roll, pitch and yaw angles were measured by a fibre optical gyroscope.

Table 1 Principal Particulars of the ONR Flare topside vessel

Length : $L_{pp}$	154.0 [m]	3.158 [m]
Breadth : $B$	19.65 [m]	0.403 [m]
Depth : $D$	15.2 [m]	0.312 [m]
Draught : $d$	5.753 [m]	0.118 [m]
Displacement : $W$	9733 [ton]	83.93 [kg]
Longitudinal position of center of buoyancy from the midship : $LCB$	6.45 [m] aft	0.132 [m] aft
Radius of gyration in pitch : $K_{yy}/L_{pp}$	0.272	0.272
Block coefficient : $C_b$	0.536	0.536
Metacentric height : $GM$	0.8095 [m]	0.0166 [m]
Natural roll period : $T_\phi$	21.11[s]	3.023 [s]

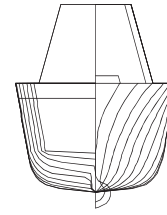


Figure 2 Body plan of the the ONR Flare topside vessel

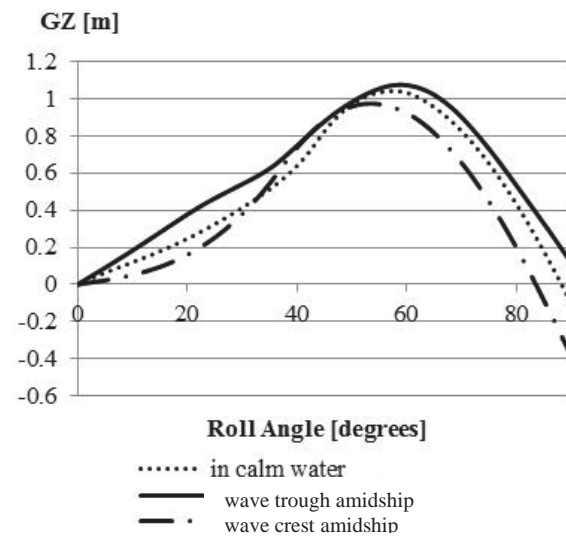


Figure 3 GZ variations of the ONR flare topside vessel in longitudinal waves whose wavelength to ship length ratio is 1.25 and the wave steepness is 0.03.

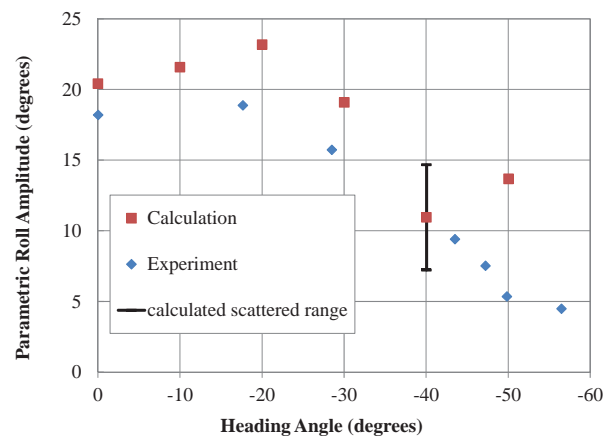


Figure 4 Steady amplitude of parametric roll in oblique waves.



The principal particulars and body plan of the subject ship are shown in Table 1 and Figure 2, respectively.

The experiment shown here is executed for regular astern waves. The wavelength to ship length ratio is 1.25 and the wave steepness is 0.03. Under this wave condition, the GZ curve of this vessel definitely changes due to longitudinal waves as shown in Figure 3. The auto pilot course ranges from 0 degrees from the wave direction to 70 degrees but no parametric roll occurred for the auto pilot course of 70 degrees. The propeller RPS is set to be 72, which corresponds to the Froude number of 0.05 in calm water. In addition, speed trials, roll decay tests and propeller open test were executed for this ship model.

#### 4. RESULTS AND DISCUSSION

The numerical results are compared with the experimental results as shown in Figure 4. Here the steady amplitude for each condition is plotted. An example of numerical runs is shown in Figure 5. In this case the roll motion is settled to a steady periodic state. The roll period is twice the pitch period, and is nearly equal to the ship natural roll period. Thus this can be judged as a typical parametric rolling. Similarly, in the auto pilot course of -30 degrees the steady periodic state was simulated as shown in Figure 6. However, in case of the auto pilot course of -40 degrees as shown in Figure 7, the calculated roll angle does not settled to a periodic state. Similar complicate response was reported by Hashimoto & Umeda (2004) with an uncoupled roll model with parametric and direct excitation. Thus this could be a future task with nonlinear dynamics.

The calculated values slightly overestimate the measured values. Good agreement between the two can be found at the heading angle of 0 degrees but some discrepancies can be found in case of oblique waves. The heading angle is rather different from the specified autopilot course. This could indicate that steady wave

forces and manoeuvring forces could have some roles.

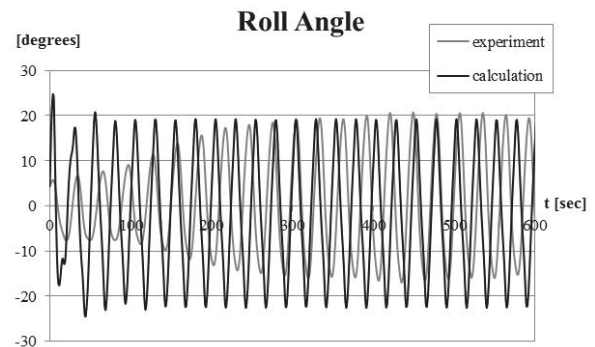


Figure 5 Time series of roll and pitch angles with the auto pilot course of -10 degrees.

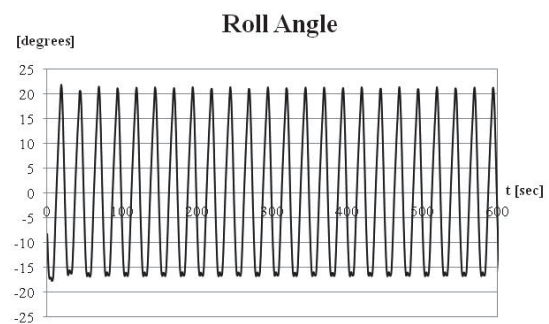


Figure 6 Time series of roll angle with the auto pilot course of -30 degrees.

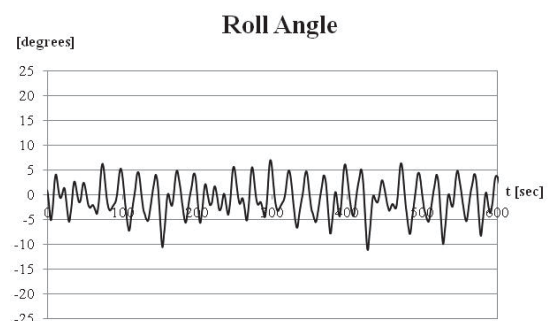


Figure 7 Time series of roll angle with the auto pilot course of -40 degrees.

The largest roll amplitude occurs at the heading angle different from head waves both



in experiment and calculation. However, when the heading angle further increases, the roll amplitude decreases. This is due to the shift of encounter frequency together with the reduction of roll restoring variation.

## 5. CONCLUSIONS

Parametric roll in regular oblique waves was realised in free-running model experiments. The 5 degrees-of-freedom numerical model slightly overestimates the experimental results. The numerical model used here includes nonlinear Froude-Krylov components, radiation / diffraction components as functions of roll angle and manoeuvring forces. The roll amplitude decreases with the increasing heading angle but the largest roll occurs with non-head waves. Non periodic roll response was found in one case of numerical simulation. Following this preliminary validation, wider validation studies in oblique waves will be executed with different ships and different wave heading in the near future.

## 6. ACKNOWLEDGEMENTS

This work was supported by JSPS (Japan Society for Promotion of Science) KAKENHI Grant Number 24360355 and 15H02327. It was partly carried out as a research activity of Goal-based Stability Criteria Project of Japan Ship Technology Research Association in the fiscal year of 2013, funded by the Nippon Foundation. The authors thank Prof. H. Hashimoto, Ms. F. Yoshiyama and N. Yamashita for their effective assistance during the work described here.

## 7. REFERENCES

- France, W.N., Levadou, M., Treacle, T.W. et al., 2003, "An Investigation of Head-Sea Parametric Roll and Its Influence on Container Lashing System", Marine Technology, 40(1), pp.1-19.
- Hashimoto, H. and N. Umeda, 2004, "Nonlinear analysis of parametric rolling in longitudinal and quartering seas with realistic modeling of roll-restoring moment", Journal of Marine Science and Technology, Vol. 9, pp. 117-126.
- Hashimoto, H. and Umeda, N., 2010, "A Study on Qualitative Prediction of Parametric Roll in Regular Head Wave", Proceedings of the 10th International Ship Stability Workshop, Wageningen, pp.295-301.
- ITTC, 2008: Recommended Procedures, Model Tests on Intact Stability, 7.5-02-07-04.
- Neves, M.A.S. and Valerio, L. 2000, "Parametric Resonance in Waves of Arbitrary Heading", Proceedings of the 7th International Conference on Stability and Operational Safety of Ships and Ocean Vehicles, Launceston, B, pp. 680-687.
- Reed, A.M., 2011, "26th ITTC Parametric Roll Benchmark Study", Proceedings of the 12th International Ship Stability Workshop, Washington D.C., pp. 195-204.
- Salvesen, N., Tuck, E.O. and O. Faltinsen, 1970, "Ship Motions and Sea Loads", Transaction of the Society of Naval Architects and Marine Engineers.
- Sanchez, N.E. and Nayfeh, A.H. 1990, "Rolling of Biased Ships in Quartering Seas", Proceedings of the 18th Symposium on Naval Hydrodynamics, Michigan.
- Umeda, N. and Y. Yamakoshi, 1989, "Hydrodynamic Forces Acting on a Longitudinally Non-symmetric Ship Under Manoeuvring at Low Speed", Journal of the Kansai Society of Naval Architects, No. 211, 127-137, (in Japanese.)
- Umeda, N. 2013, "Current Status of Second Generation Intact Stability Criteria", Proceedings of the 13th International Ship Stability Workshop, Brest, pp. 138-157.



Watanabe, Y., 1934, “On the Dynamical Properties of the Transverse Instability of a Ship due to Pitching”, Journal of the Society of Naval Architects, Vol. 53, pp. 51-70 (in Japanese)

This page is intentionally left blank